ChemPubSoc Europe

DOI: 10.1002/open.201800078

Open Access ChemistryOPEN Full Papers

The Effect of Polymer Structures on Complete Degradation: A First-Principles Study

Yu Zhu,[a, b] Depeng Zhang,[a, b] Zhanwen Zhang,[a, c] and Zhigang Wang*[a, b]

The widespread application of hydrocarbon polymer materials has spurred an increasing interest in the study of their dissociation mechanism, which is related to key issues such as environmental protection. In this work, the last-step dissociation characteristics of carbon chain polymers were investigated. By using density functional theory, we considered all possible structures, including three typical normal linkage polymers and four typical abnormal linkage ones. In these structures, it can be found that the energy barrier required for the complete degradation of chain-end saturated and unsaturated polymers are in the range of 3.42 to 4.78 eV and 0.35 to 1.31 eV, respectively. It shows that the unsaturated polymer is easier to degrade. Interestingly, as for three linkages of the polymer, the calculated results further suggest that the energy barrier of head-to-head, head-to-tail, and tail-to-tail linkages of the polymer dissociating to produce the monomer increase, no matter if the chain-end is saturated or not. Therefore, we form a regular understanding of how to achieve the complete degradation of the polymer. In addition, analyses of the bond characteristics and electronic structures agree with the results of the energy barrier measurements. Meanwhile, the spin population analysis presents an obvious net spin transfer process in depolymerization reactions. We hope that the current results can provide a basic insight into polymer degradation.

1. Introduction

As an atomic-level process, polymer degradation is an extremely important subject in the field of environmental protection[1] and has received a lot of attention. In the past, most studies have focused on the normal linkages of hydrocarbon polymers to study the idealized degradation reaction process. In fact, we have noticed that the polymer abnormal linkage or chain-end saturation will obviously affect the stability of polymer chain,[2] resulting in the uncertainty of degradation. That should be taken seriously. However, it is not clear at atomic level, for which we hope to understand the mechanism in this work.

According to the different external factors that polymer suffer from, there are three major classes of degradation, namely, photodegradation, thermal degradation, and biodegradation.[3] Actually, the polymer chain depolymerization can be seen as the inverse process of polymerization.[4] Hence, the study of degradation is also important to the understanding of polymer synthesis. For example, the monomers can be recycled by polymer degradation to synthesize new polymers.[5] Normally, the chain end of the polymer will be saturated with a functional group to enhance the stability of the system in use processes. Concomitantly, it will have an evident impact on polymer degradation,[2b] which is something that remains unclearly. In addition, the degree of difficulty of polymer degradation could also be influenced by the different ways that the monomer unit is connected,[6] including head-to-tail (H-T), head-to-head (H-H), and tail-to-tail (T-T) linkages.[7]

To date, experimental techniques have been greatly improved. For instance, the geometric properties of reactants and products can be obtained by various spectroscopy methods,[8] and the formation of radicals during polymer degradation also can be detected.[9] However, as the degradation process may have multiple reaction channels, in situ observation is hard to obtain experimentally. Consequently, it is necessary to understand the mechanism of polymer degradation from a theoretical perspective. In this work, we selected a typical hydrocarbon polymer, poly-α-methylstyrene (PAMS), for the calculation models and to study the effect of polymer structures on complete degradation through potential energy surfaces, bond characteristic, spin population, and other calculations.

[a] Y. Zhu, D. Zhang, Z. Zhang, Prof. Z. Wang
Institute of Atomic and Molecular Physics, Jilin University
Changchun, 130012 (P. R. China)
E-mail: wangzg@jlu.edu.cn

[b] Y. Zhu, D. Zhang, Prof. Z. Wang
Jilin Provincial Key Laboratory of Applied Atomic and Molecular Spectroscopy, Jilin University
Changchun 130012 (P. R. China)

[c] Z. Zhang
China Academy of Engineering Physics
Mianyang 621900 (P. R. China)

Supporting Information and the ORCID identification number(s) for the author(s) of this article can be found under: https://doi.org/10.1002/open.201800078.

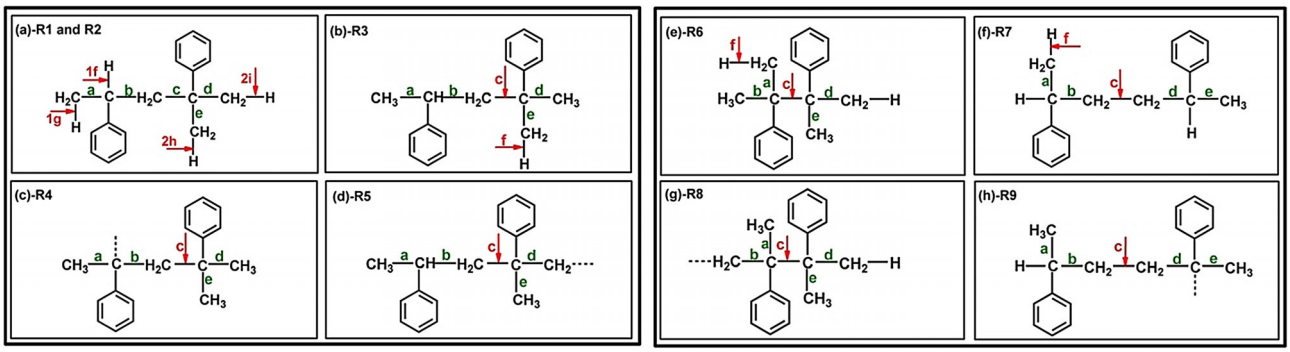

Figure 1. Geometric structures of nine chain-like PAMS dimers. Among them, R1 and R2 represent C-end and CH_2-end dissociation paths that produce H_2. R3 represents the reaction of the dissociation of the monomer AMS. The C-unsaturated end and CH_2-unsaturated end dissociation paths that produce AMS are marked as R4 and R5, respectively. R6 and R7 represent the H-H reaction and T-T reactions, respectively. The H-H reaction with one unpaired electron at the end and the T-T reaction with one unpaired electron at the end are marked R8 and R9, respectively. The location of red arrows denotes the bonds breaking on the same degradation path. The green letters represent the corresponding bonds.

Computational Methods

We studied all possible structures of the PAMS dimer, including three typical normal linkages and four abnormal linkages, which had nine depolymerization reactions. As shown in Figure 1, the nine chain-like PAMS dimers were marked R1–R9.

In this study, the extreme points [including reactants, transition states (TSs), and products] were optimized by using the generalized gradient approximation (GGA) with empirical dispersion-corrected density functional theory (DFT-D3) at the B3LYP/ 6–31 + G(d,p) level[10] in Gaussian 09.[11] Based on the optimized geometries, the frequency calculations were performed at the same level. The number of imaginary frequencies was used to confirm that the structure was a stable point (zero) or a TS (one). Meanwhile, zero-point-energy (ZPE) corrections were also considered. The intrinsic reaction coordinate (IRC)[12] was calculated to ensure the reliability of reaction process (see Figure S1 in the Supporting Information).

2. Results and Discussion

The potential energy curves of all reactions are presented in Figure 2. Initially, the three typical chain-end saturated PAMS dimers were studied, and we found that the PAMS dimer chain dissociation product H_2 has two reaction paths (R1 and R2). It can be see that the energy barriers of R1 and R2 are about 4.53 and 4.99 eV, respectively, indicating that the C-end dissociation reaction is prone to occur. More importantly, in addition to the above dissociation reactions, the H transfer of the methyl on the main chain can realize the dissociation of the monomer AMS (R3). The energy barrier of R3 is 4.20 eV. From the potential energy curves of reactions R6 and R7, we can see that their energy barriers are about 3.42 and 4.78 eV, respectively. These results suggest that the H-H reaction occurred preferentially. Then, we also studied the four typical chain-end unsaturated PAMS dimers. The energy barrier of reactions R4 and R5 are about 0.79 and 0.86 eV, respectively, showing that the dissociation of the monomer AMS is more likely to occur at the C-unsaturated end. Reactions R8 and R9 need to overcome the energy barrier of 0.35 and 1.31 eV, respectively. It declares that the H-H reaction with one unpaired electron at the end may easily dissociate. Furthermore, it is also found that

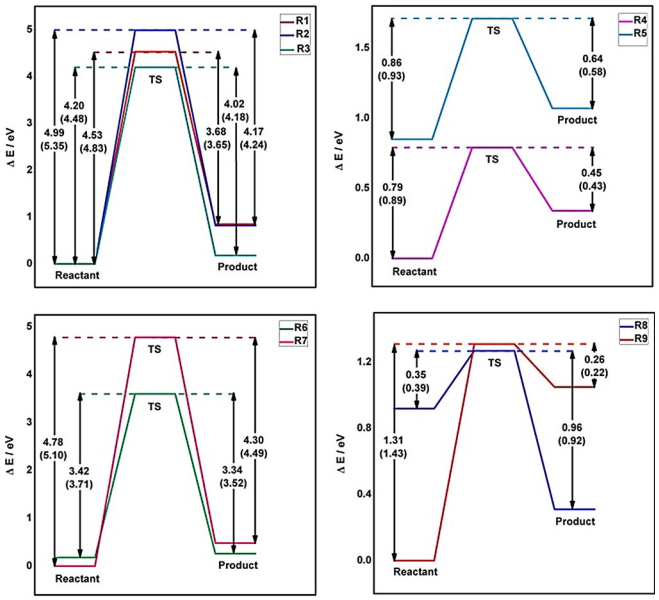

Figure 2. Potential energy curves of nine typical dissociation reactions. The energy values were obtained based on the sum of the total energy and the zero-point vibrational energy, and the energy value in brackets represents the total energy.

unsaturated PAMS dimer is more likely to degrade compared to the saturated one. In addition, the energy barriers of H-H, H-T, and T-T linkage PAMS dimers, dissociating to produce the monomer, increase no matter if the chain-end is saturated or not. It is worth mentioning that, when the ends are both unsaturated, the energy barrier of PAMS dimer for degradation reaction can be as low as 0.03 eV,[13] which is far below that of the reactions discussed above. As it is easy to degrade, we did not study this structure with one dangling bond at each end in this work. It is important to note that R8 is an exothermic reaction, whereas the other eight reactions correspond to the endothermic reactions.

The corresponding TSs of the nine reactions are shown in Figure S2. As for degradation reactions (R1, R2) that produce H_2, the TSs are broken at the two C–H bonds at the end of the

chain. In the degradation reactions that produce the monomer, the TSs are all broken at the C–C bond in the linkage site of the monomer. In particular, for the complete degradation of saturated dimers, the TSs are also broken at the C–H bond at the chain end in addition to the above C–C bond (for more details, see Figure 1).

To achieve a better understanding of the relevant bond characteristics, we summarized the bond orders and bond lengths of the reactants in seven reactions. The bond orders and bond lengths of broken C–C bond were carried out (see Table 1). For the R3, R6, and R7 reactants, the bond order of 6c (0.93) is weaker than that of 3c (0.97) and 7c (1.02). The bond length of 6c (1.62) is longer than that of 3c (1.57) and 7c (1.54). These results indicate that the 6c bond is easily broken and that the H-H reaction may preferentially occur among the dissociation reactions of chain-end saturated PAMS dimers. For the R4, R5, R8, and R9 reactants, the bond orders increase in the order of 8c (0.92), 4c (0.94), 5c (0.97), and 9c (1.04), and the corresponding bond lengths are decrease. This suggests that the bond of the H-H linkage site (8c) is weakest and the bond of the T-T linkage site (9c) is hardest to break. These bond properties strongly support the results that the monomer is relatively easy to dissociate at the H-H abnormal linkage site. In addition, the T-T reaction is most difficult and unlikely to occur. Moreover, the results of bond property analyses conform to the analyzed results of the energy barrier measurements.

Table 1. The bond orders and bond lengths of broken C–C bonds in seven dissociation reactions that produce the monomer. Here, the "c" represents the broken C–C bond. 6c and 8c are both H-H linkage sites. 7c and 9c are T-T linkage sites. (The specific location can be seen Figure 1).

c	R3	R4	R5	R6	R7	R8	R9
Bond order	0.97	0.94	0.97	0.93	1.02	0.92	1.04
Bond length [Å]	1.57	1.58	1.57	1.62	1.54	1.62	1.50

Depolymerization will lead to the process of net spin migration.[6a] Thus, we further explored the degradation reaction mechanism from the perspective of the spin population. Among these reactions, the reactants, TSs, and products of reactions R1–R3, R6, and R7 are all closed-shell electronic structures, and they do not have a net spin. However, the structures of the other four reactions are open-shell electronic structures, which are spin-polarized. Their net spin distributions are shown in Figure 3. It can be found that, in the reactants, the net spins are mainly distributed at the unsaturated end of the chain. In the TSs, the opposite net spin electrons are found in the area of the broken C–C bond, owing to stretching of the C–C bond. For the products, the net spins on dissociated monomer self-coupled into a closed-shell electronic structure. Meanwhile, the net spin electrons on the surplus main chain still maintain free-radical characteristics.

To acquire the electronic structures of reactants in reactions R3 (R1, R2), R6, and R7, we studied the frontier molecular orbitals (MOs) of them.[14] The reactants of reactions R3, R6 and R7

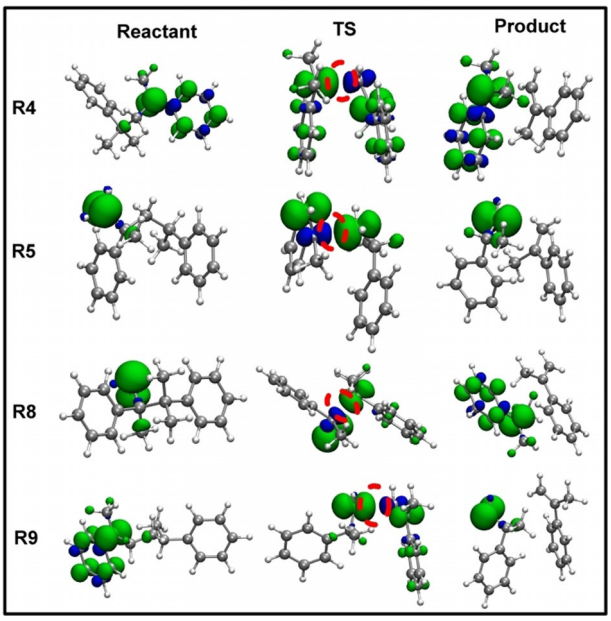

Figure 3. The spin population of four spin-polarized reaction paths. The green and blue areas of the structures represent the net spin up and down, respectively. Isovalue = 0.005.

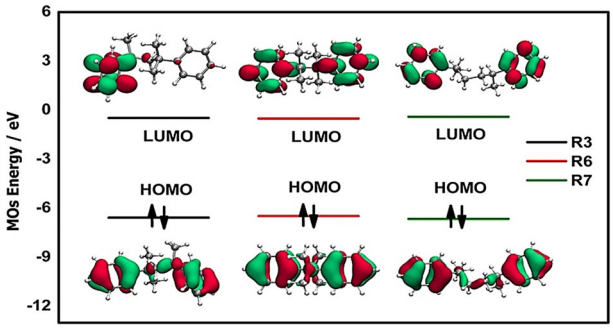

Figure 4. The selected frontier MOs of the stable reactants in reactions R3 (R1, R2), R6, and R7. The reactants of reactions R1, R2 and R3 are the same. Isovalue = 0.035.

are all chain-end saturated PAMS dimers. Figure 4 shows their frontier MOs. The HOMO (highest occupied molecular orbital) and the LUMO (lowest unoccupied molecular orbital) of the R6/R7 reactant are mainly localized at the H-H/T-T linkage sites of the chain and the nearby benzene group. The HOMO and LUMO of R3 (R1, R2) have similar characteristics. Meanwhile, we can see that the reactants HOMO–LUMO gap for R7 (6.25 eV), R3 (6.09 eV), and R6 (5.97 eV) are decreasing. It shows that the H-H linkage site in reaction R6 has a high chemical reactivity, which also explains why the energy barriers of R6, R3, and R7 are increasing. In addition, the TSs frontier MOs of R1, R2, and R3 were also studied (see Figure S3). It can be seen that the HOMO and LUMO are mainly located at positions near the broken bonds. Furthermore, the TSs HOMO–LUMO gap of R2 (3.70 eV), R1 (3.50 eV), and R3 (2.87 eV) are decreasing, suggesting that the position of the broken bonds in reaction R3 has a high chemical reactivity. Therefore, the

energy barrier of PAMS dimers dissociating to produce H_2 and AMS monomer is decreasing.

3. Conclusions

In this work, the degradation mechanism of three typical normal linkage and four abnormal linkage PAMS were investigated. For chain-end saturated structures, calculations of the energy barriers show that the H-H dissociation reaction occurs relatively easily. In chain-end unsaturated structures, the calculated results indicate that the H-H reaction with one unpaired electron at the end may easily dissociate. Furthermore, from different dissociation reactions, we also found that the energy barrier for H-H, H-T, and T-T linkage polymer dissociation to produce the monomer increases, no matter if the chain-end is saturated or not. The chain-end unsaturated structure is easier to degrade than the chain-end saturated one. In addition, the degradation of PAMS also follows other channels, which can produce H_2. The H-H reaction with one unpaired electron at the end corresponds to an exothermic reaction. But, the other eight reactions are endothermic reactions. Analyses of bond characteristics and electronic structures are in agreement with the results of energy barrier measurements, and the spin population analysis presents an interesting net spin transfer process in depolymerization reactions of four spin-polarized structures. We hope the present theoretical study could provide some reference for the complete degradation of polymers.

Acknowledgements

We would like to thank Rui Wang, Weiyu Xie, and Jianpeng Wang for stimulating discussions. This work was supported by the National Science Foundation of China (grant number 11374004 and 11674123). Z.W. also acknowledges the High-Performance Computing Center of Jilin University.

Conflict of Interest

The authors declare no conflict of interest.

Keywords: chain-end saturation · degradation · first-principles calculations · hydrocarbons · polymers

[1] a) V. Delplace, J. Nicolas, *Nat. Chem.* **2015**, *7*, 771–784; b) J. M. Garcia, M. L. Robertson, *Science* **2017**, *358*, 870–872.
[2] a) Y. Nagasaki, N. Yamazaki, M. Kato, *Macromol. Rapid Commun.* **1996**, *17*, 123–129; b) H. Nakatani, S. Suzuki, T. Tanaka, M. Terano, *Polym. Int.* **2007**, *56*, 1147–1151; c) H. Nakatani, D. Kurniawan, T. Taniike, M. Terano, *Sci. Technol. Adv. Mater.* **2008**, *9*, 024401.
[3] a) S.-i. Kuroda, I. Mita, K. Obata, S. Tanaka, *Polym. Degrad. Stab.* **1990**, *27*, 257–270; b) A. Göpferich, *Biomaterials* **1996**, *17*, 103–114; c) K. Chrissafis, *J. Therm. Anal. Calorim.* **2008**, *95*, 273–283.
[4] V. Deguine, M. Menasche, P. Ferrari, L. Fraisse, Y. Pouliquen, L. Robert, *Int. J. Biol. Macromol.* **1998**, *22*, 17–22.
[5] a) D. D. Jiang, C. A. Wilkie, *J. Polym. Sci. Part A* **1997**, *35*, 965–973; b) R. Qi, Z. Chen, C. Zhou, *Polymer* **2005**, *46*, 4098–4104.
[6] a) T. Yu, Y. Gao, B. Wang, X. Dai, W. Jiang, R. Song, Z. Zhang, M. Jin, Y. Tang, Z. Wang, *Chemphyschem* **2015**, *16*, 3308–3312; b) T. Yu, C. Tian, X. Liu, J. Wang, Y. Gao, Z. Wang, *J. Electron. Mater.* **2017**, *46*, 3933–3937.
[7] a) M. Tanaka, T. Shimono, Y. Yabuki, T. Shono, *J. Anal. Appl. Pyrolysis* **1980**, *2*, 207–215; b) Z. Doležal, R. Kubinec, J. Sedláček, V. Pacáková, J. Vohlídal, *J. Sep. Sci.* **2007**, *30*, 731–739.
[8] A. G. Kalampounias, K. S. Andrikopoulos, S. N. Yannopoulos, *J. Chem. Phys.* **2003**, *118*, 8460–8467.
[9] M. Lucarini, G. F. Pedulli, M. V. Motyakin, S. Schlick, *Prog. Polym. Sci.* **2003**, *28*, 331–340.
[10] a) C. Lee, W. Yang, R. G. Parr, *Phys. Rev. B* **1988**, *37*, 785–789; b) B. Miehlich, A. Savin, H. Stoll, H. Preuss, *Chem. Phys. Lett.* **1989**, *157*, 200–206; c) A. D. Becke, *J. Chem. Phys.* **1993**, *98*, 5648–5653.
[11] Gaussian 09, Revision D.01, M. J. Frisch, G. W. Trucks, H. B. Schlegel, G. E. Scuseria, M. A. Robb, J. R. Cheeseman, G. Scalmani, V. Barone, B. Mennucci, G. A. Petersson, H. Nakatsuji, M. Caricato, X. Li, H. P. Hratchian,A. F.Izmaylov, J. Bloino, G. Zheng, J. L. Sonnenberg, M. Hada, M. Ehara, K. Toyota, R. Fukuda, J. Hasegawa, M. Ishida, T. Nakajima, Y. Honda, O. Kitao, H. Nakai, T. Vreven, J. A.Montgomery, Jr., J. E. Peralta, F. Ogliaro, M. Bearpark, J. J. Heyd, E. Brothers, K. N. Kudin, V. N. Staroverov, R. Kobayashi, J. Normand, K. Raghavachari, A. Rendell, J. C. Burant, S. S. Iyengar, J. Tomasi, M. Cossi, N. Rega, J. M. Millam, M. Klene, J. E. Knox, J. B. Cross, V. Bakken, C. Adamo, J. Jaramillo, R. Gomperts, R. E. Stratmann, O. Yazyev, A. J. Austin, R. Cammi, C. Pomelli, J. W. Ochterski, R. L. Martin, K. Morokuma, V. G. Zakrzewski, G. A. Voth, P. Salvador, J. J. Dannenberg, S. Dapprich, A. D. Daniels, Ö. Farkas, J. B. Foresman, J. V. Ortiz, J. Cioslowski, D. J. Fox, *Gaussian, Inc., Wallingford CT* **2009**.
[12] a) K. Fukui, *J. Phys. Chem.* **1970**, *74*, 4161–4163; b) C. Gonzalez, H. B. Schlegel, *J.phys.chem* **1990**, *94*, 5523–5527.
[13] T. Yu, J. Wang, W. Jiang, Z. Zhang, Y. Zhu, Y. Tang, Z. Wang, *Chemistryselect* **2018**, *3*, 2553–2557.
[14] a) Z. Zhou, R. G. Parr, *J. Am. Chem. Soc.* **1990**, *112*, 5720–5724; b) J.-i. Aihara, *Phys. Chem. Chem. Phys.* **2000**, *2*, 3121–3125.

Received: May 3, 2018

